

Extraction of Sizes and Velocities of Spray Droplets by Optical Imaging Method

Yeonjun Choo, Boseon Kang*

*Department of Mechanical Engineering, Chonnam National University,
300, Yongbong-Dong, Buk-Gu, Gwangju 500-757, Korea*

In this study, an optical imaging method was developed for the measurements of the sizes and velocities of droplets in sprays. Double-exposure single-frame spray images were captured by the imaging system. An image processing program was developed for the measurements of the sizes and positions of individual particles including separation of the overlapped particles and particle tracking and pairing at two time instants. To recognize and separate overlapping particles, the morphological method based on watershed segmentation as well as separation using the perimeter and convex hull of image was used consecutively. Better results in separation were obtained by utilization of both methods especially for the multiple or heavily-overlapped particles. The match probability method was adopted for particle tracking and pairing after identifying the positions of individual particles and it produced good matching results even for large particles like droplets in sprays. Therefore, the developed optical imaging method could provide a reliable way of analyzing the motion and size distribution of droplets produced by various sprays and atomization devices.

Key Words : Optical Imaging Method, Morphological Method, Spray Droplet, Particle Tracking Algorithm

Nomenclature

- D_E : Euclidian distance function
 M : Number of possible match points in the second pulse
 P_{ij} : Match probability that X_i would coincide to Y_j
 P_i^* : No-match probability that X_i has no-corresponding Y_j
 T_m : Threshold radius for maximum movement
 T_n : Threshold radius for neighborhood
 T_q : Threshold radius for quasi-solidity
 X_i : Particle in the first pulse image
 Y_j : Particle in the second pulse image

Superscripts

- (n) : Number of iteration step
 \sim : Non-normalized probability

1. Introduction

Many different techniques and instruments have been employed in the research upon spray and atomization to investigate spray characteristics, such as the sizes and velocities of droplets, and the spray patterns produced by different atomization devices. Techniques of droplet sizing may be classified into three broad categories : mechanical, electrical, and optical. In particular, a variety of optical systems for spray analysis has been developed in recent years. Each system has its own advantages and limitations, but all benefit because of their non-intrusive natures. The PDPA (Phase Doppler Particle Analyzer), one of the most widely used optical systems, measures droplet sizes and velocities simultaneously by using

* Corresponding Author,

E-mail : bskang@chonnam.ac.kr

TEL : +82-62-530-1683; **FAX :** +82-62-530-1689

Department of Mechanical Engineering, Chonnam National University, 300, Yongbong-Dong, Buk-Gu, Gwangju 500-757, Korea. (Manuscript **Received** December 1, 2003; **Revised** April 2, 2004)

phase differences between detectors and a doppler signal obtained from scattered light by passing droplets through a fringed control volume. However, its use is inherently limited in denser spray regions, where liquid elements are rather large and non-spherical. In addition, it is the point-measurement technique and information on overall spray structure is beyond the capability of this type of laser instrument.

On the other hand, spray characterization by the optical imaging method is accurate, simple and economic, and provides details of droplet characteristics and allows the visualization of spray patterns. Moreover, rapid progress in the development of the elements of the required system hardware, such as high performance CCD cameras and computers has resulted in remarkable increases in the efficiency of image processing procedure. Therefore, techniques of particle characterization based on imaging methods have significantly extended their fields of application.

When the optical imaging method is used to simultaneously measure sizes and velocities of solid/liquid particles in liquid/gaseous flows, the main issues are identification of particles and particle tracking. For particle identification, the proposed methods by previous researchers can be grouped into two major categories; the gray-level-based approach and the geometrical approach. Among the gray-level-based approach, the global threshold method was proposed by Lee et al. (1991), Kim (2000), and Sudheer and Panda (2000). This method uses the cumulative histogram of each pixel's gray level to find out a single threshold value that segments the foreground (particles) and the background. This method, however, is influenced by the image quality such as foreground concentration, background uniformity and so on. Some researchers (Kim and Kim, 1994; Kim et al., 1999; Kho et al., 2001) used the local threshold method to determine an appropriate normalized gray value from the relationship between the gray level of a particle and the background. Nishino et al. (2000) and Kim and Lee (2002) used the gray level gradient around the edge of particle to define

the boundary. The geometrical approach can be effectively used for the separation of overlapping particles. Several researchers (Crida and Jager, 1997; Kim and Lee, 2002; Kruis et al., 1994) used a sophisticated method, so-called Hough transform that is especially useful in separating the overlapping particles. The Hough transform is a standard tool in image analysis that allows recognition of global patterns in an image space by recognition of local patterns in a transformed parameter space. The boundary curvature detection method (Kim et al., 2001) finds out the abrupt changes of curvature at the contact points of the overlapped particle image. Kim et al. (1999) used the smallest convex hull image of objects that contains all points such a way that any arbitrary two points inside the convex hull can be connected by a straight line. Two farthest points from the convex hull are determined as two separation points of overlapped particles. The process time of this method is much shorter than any other techniques but it possesses some limitations in analyzing the multiple-overlapped particles. The watershed separation (Sonka et al., 1999), which is a type of morphological segmentation, is a frequently used method for particle separation. The separation result is comparatively good except for heavily overlapped particles or overlapping of particles with a large difference in sizes. In this study, therefore, the watershed separation was adopted first to perform the fundamental separation including separation of overlapping by more than two particles, and this was followed by separation based on the perimeter and the convex hull of the image to improve the results obtained by the watershed separation.

The measurement of particle velocities by the optical imaging method are usually restricted to cases where particles do not move appreciably in the depth direction, thus allowing particle velocities to be considered as two-dimensional. Many techniques have been suggested to determine particle velocities from double-exposed particle images. Some well-known methods are auto-or cross-correlation, statistical methods, neural network methods, nearest neighbor particle image

matching (Labonte, 2000), fuzzy algorithm (Shen et al., 2001), and the match probability algorithm (Baek and Lee, 1996; Ballard and Brown, 1982; Lecuona et al., 2000). Of these, the match probability algorithm produces very high matching accuracies, even though the concept itself is straightforward.

In this study, the sizes and velocities of droplets produced by a commercial spray nozzle were measured using an optical imaging method from digital images of regions within sprays. Double-exposure, single-frame spray images with short pulse intervals were captured by an image capturing system. Sizes and positions of the individual particles were obtained after the appropriate image processing, which included the separation of the overlapped particles based on the watershed segmentation as well as on the perimeter and the convex hull of the image. Using this information, particle velocities were determined by applying the match probability algorithm.

2. Image Capturing System

The optical system used to acquire double pulse images of liquid droplets in a water spray formed by a commercial full-cone nozzle was Particle Motion Analysis System (V-tek Co.); a schematic of the equipment is shown in Fig. 1. The region of interest was back-lit using a dual spark light source of very short pulse duration (50 ns). This allowed fast moving objects to be frozen and allowed consecutive double sparks to be fired at controllable intervals (1 μ s or greater) to determine velocities. A diffuser was inserted between the light source and the region

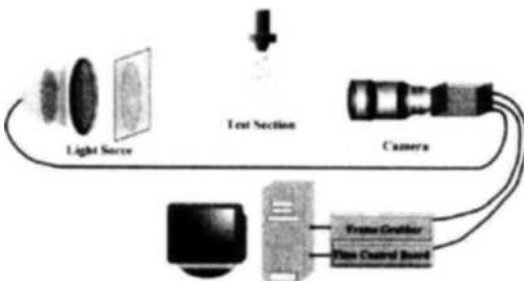


Fig. 1 Particle image capturing system

of interest to provide a uniform background. To obtain much-magnified images, a field lens was used in addition to the long working distance micro-optics attached to the CCD camera (636×476 pixels). Captured images were stored in a PC equipped with a frame grabber and a time control board to ensure synchronization between the camera and the light source.

3. Image Processing Procedures

A typical spray image acquired by the image capturing system is shown in Fig. 2. Various sized spherical and elliptical droplets are typically presented in a spray. The examined region was 7.95 by 5.95 mm and one pixel corresponded to 12.5 μ m. The equivalent diameter of the largest droplet was 235.6 μ m. The droplet images of the first and second pulses are distinguished by gray values caused by the intensity differences of the light pulses. The droplet overlapping occurred between droplets at each pulse as well as at different pulses. As shown in Fig. 3, the image processing procedure used to obtain droplet sizes and velocities from this kind of spray images consists of the following steps; 1) the separation of overlapping droplets, 2) the separation of double pulse images into images corresponding to each light pulse, 3) the application of the particle tracking algorithm.

To enhance the image quality for further processing, some pre-processing works such as the

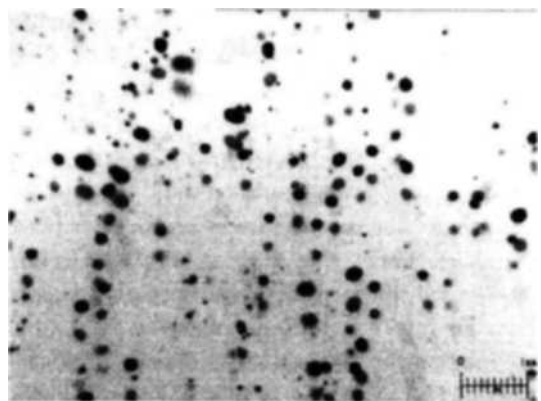


Fig. 2 Typical double exposure image of spray droplets

median filtering to reduce salt and pepper noises and the hole filling of the bright spot in the center of droplet image were performed first. Then, the image was binarized into droplets and background by thresholding. Global thresholding produces different separation results depending on the local background intensity because this is usually not uniform over the region of interest. To avoid this problem, the whole region of interest was divided into smaller areas, the sizes of which were dependent on the location of the droplet centers found by global thresholding. Local thresholding, within the smaller areas results in a more accurate separation of droplets from the background. The Otsu's method (1979) that divides statistically the histogram into two classes of Gaussian distribution for the foreground and the background was adopted to determine the global and local threshold values.

Ahead of the separation process, the overlapped particles should be differentiated from the single particles. The criteria used in identifying the overlapped particles were elongatedness, compactness, and solidity. These parameters are defined as functions of geometric properties of binarized particles, as shown in Fig. 4. The associated

definitions are as follows :

$$\text{elongatedness} = \frac{\text{equivalent length}}{\text{equivalent breadth}} \quad (1)$$

$$\text{compactness} = \frac{(\text{perimeter of overlapped area})^2}{\text{overlapped area}} \quad (2)$$

$$\text{solidity} = \frac{\text{convex hull area}}{\text{overlapped area}} \quad (3)$$

All three criteria have similar capabilities in identifying the overlapped particles, but elongatedness was selected because it was more sensitive to the degree of overlapping and less dependent on the size of object than the other criteria. As shown in Fig. 4, elongatedness is always greater than one and approaches one as the particle becomes more spherical, thus its value deviates from one for overlapping particles.

Next, the centers of individual particles are determined by using a Euclidean distance function. As described below, the Euclidean distance function represents the distance between the pixel (i, j) inside a particle and a pixel (h, k) at nearest boundary.

$$D_E[(i, j), (h, k)] = \sqrt{(i-h)^2 + (j-k)^2} \quad (4)$$

Figure 5 shows changes in pixel values after applying the Euclidean distance function. The

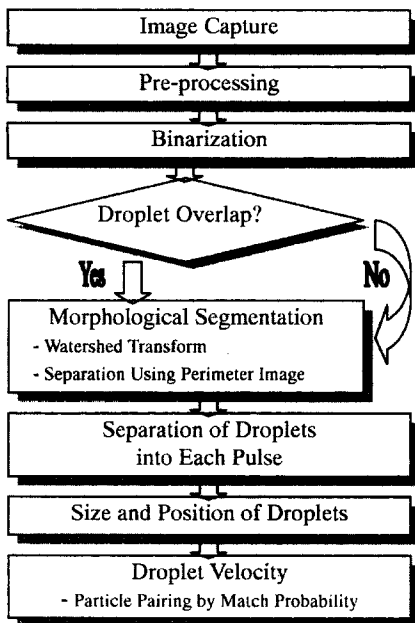


Fig. 3 Flow chart of image processing procedure

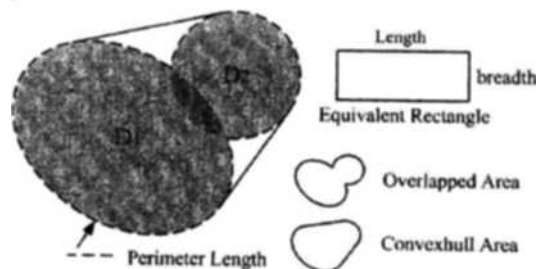


Fig. 4 Geometric terminology for overlapped particles

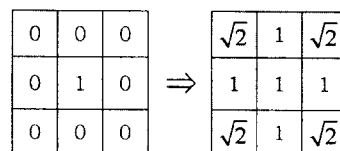


Fig. 5 Euclidean distance transform

images are represented by local brightness differences after applying this transformation. The brightest points correspond to the centers of the individual particles because a center is the farthest point from the boundary of a particle.

After binarization and center finding, the overlapped droplets are separated. The problem of separating the overlapped particles is a common problem in particle dynamics analysis by image processing so several partial solutions have been suggested so far, as mentioned in the introduction. In this study, the watershed segmentation was adopted first and this was followed by separation based on the perimeter and the convex hull of the image to obtain better separation results. The detailed separating procedure for overlapped particles using the perimeter and the convex hull of the image is shown in Fig. 6. Figure 6(a) is the separated image of four particles obtained by using the watershed transform, and shows local maximum as their centers. As can be seen

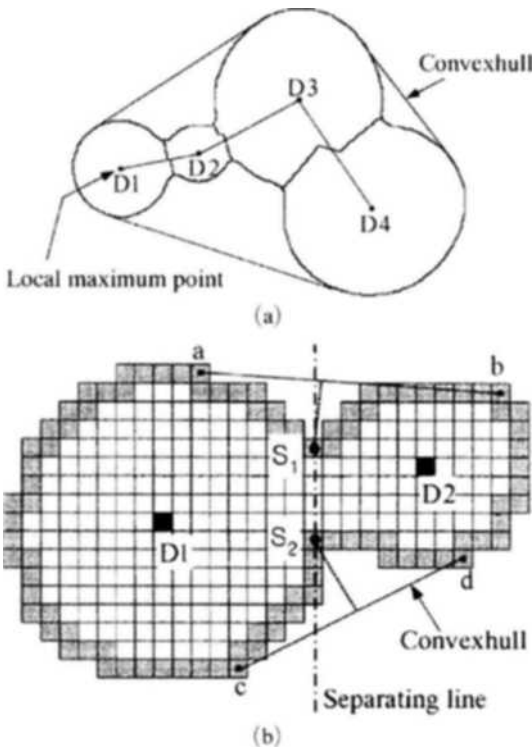


Fig. 6 Separation of overlapped particles using the perimeter and the convex hull of the image

in the figure, the watershed segmentation transform depends greatly on the areas of individual particles, and the degree of overlapping. It sometimes generates unsatisfactory separating lines like those separating D2-D3 and D3-D4 in Fig. 6(a). Figure 6(b) shows the separation procedure applied to two adjacent particles ($D1, D2$) using the perimeter and the convex hull of the image. The convex hull of overlapped particles consists of points $a, b, c,$ and d . The two points $S1$ and $S2$ are the furthest points in the perimeter of the image from the lines ab and cd , respectively. A line connecting these two points is used as the separation line in the second stage of the separation. The same method was applied to the other overlapped particles ($D2$ and $D3, D3$ and $D4$).

A typical result of the image processing procedure up to the overlapped droplet separating step using the morphological segmentation is shown in Fig. 7 by step. The binarized image of droplets and background obtained by local thresholding is shown in Fig. 7(b) for the original droplets shown in Fig. 7(a). Figure 7(c) represent the perimeter of the image in Fig. 7(b), and Fig. 7(d) was produced by applying the Euclidean distance function to the image in Fig. 7(b), and then reversing the intensity. The brightest points correspond to the centers of individual particles. Figure 7(e) represents the local maximum in the image of Fig. 7(d) after Euclidean distance transformation, and Fig. 7(f) represents the result of applying the boolean operation $NOT [(d) AND (e)]$. The watershed segmentation transform was then applied to the image of

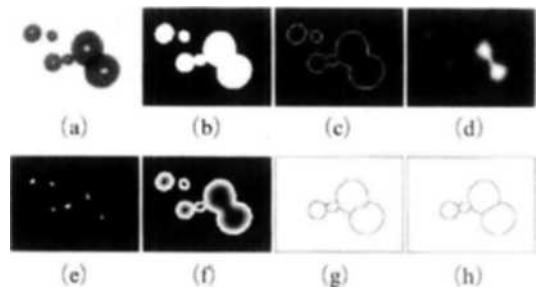


Fig. 7 Morphological segmentation procedure for overlapped particles

Fig. 7(f) producing the image shown in Fig. 7 (g). One more step of separation was performed using the perimeter and the convex hull of the image and the separation result is shown in Fig. 7(h). Much improved consequences were obtained than solely applying Watershed transform.

After binarizing the image into droplets and background, and separating the overlapping droplets, the double pulsed image should be separated into two images frozen by each light pulse prior to applying the particle tracking algorithm. Separation was possibly achieved because of different light intensities between the first and second light pulses. Threshold value used to divide droplet images into first and second pulse images was determined by the gray value histogram of the original image. Using this threshold value, the droplets are divided into first and second pulse images. For the purpose of effective calculation in the process of particle pairing, the threshold values were determined such that the number of droplets in the first pulse was always smaller than the number in the second pulse.

4. Particle Tracking Algorithm

Once the sizes, geometric characteristics, and positions of individual particles have been obtained, the next stage involves the application of the particle tracking algorithm to find the particle pairs. Particle velocities are calculated based on these pairings. In the present work, the Baek and Lee (1996)'s match probability algorithm was adopted as the particle tracking algorithm.

4.1 Basic background of the match probability algorithm

Various methods that use particles as flow tracers and obtain flow field by analyzing particle images have been suggested and developed since 1980. Adrian (1991) termed these above methods the Pulsed-Light Velocimetry (PLV) and categorized as PTV (Particle Tracking Velocimetry), PIV (Particle Image Velocimetry), and LSV (Laser Speckle Velocimetry) according to the particle density. The PIV method does not

consider individual particles in the interrogation region, but deduces a representative velocity for this region by statistically correlating the positions of particles at two instances in the interrogation region. The density of particles is relatively high and the high resolution of images used to measure individual particle sizes doesn't need to be used. On the other hand, PTV method is used to determine the velocities of individual particles at low particle density. In the research fields involving sprays or two-phase flow that require information on size and velocity, the PTV method is preferred, and high resolution images should be used. The PTV method was selected in this study because it provides particle size and velocity data.

The most important aspect of the PTV method is the means of obtaining data on pairs of images of the same particles in two time frames. Among the several algorithms used for this purpose, and which were briefly mentioned in the introduction, Baek and Lee (1996)'s match probability algorithm was adopted in the present study, because it generates very accurate pairing results, though the theory and the procedure are comparatively straightforward. The match probability algorithm repetitively evaluates the probability that candidates for the pairs are from the same particles, and then pairing is done between particles showing the highest probability. To apply this algorithm, the following basic assumptions related to particle movement phenomena are required.

- (1) The maximum distance moved is constrained by the maximum particle velocity.
- (2) Velocity changes of small particles during the short time interval are small.
- (3) Neighboring particles have similar movements.
- (4) The probability that two particles at different positions will meet at one point during the time interval is low.

A more detailed description of the algorithm can be found in Baek and Lee (1996), Ballard and Brown (1982), and Lecuona et al. (2000).

Figure 8 shows several parameters used by the algorithm, based on the above assumptions.

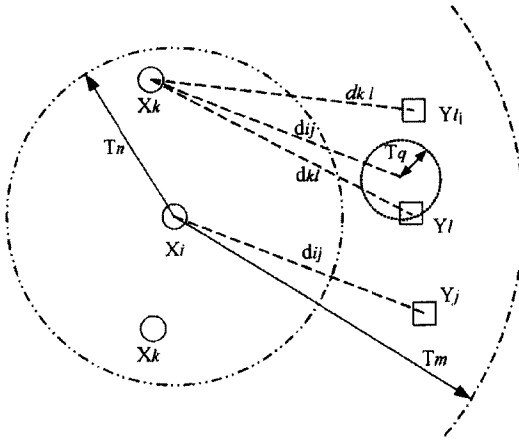


Fig. 8 Particle tracking algorithm by neighboring match probability

According to the maximum velocity assumption, the radius T_m is obtained by multiplying the possible maximum particle velocity in the first pulse by the pulse interval, and restricts candidate particles in the second pulse, Y_j , to the vicinity of particle, X_i . The radius T_n restricts particles around X_i , which satisfy the quasi-solidity assumptions (3) and (4). Namely, it identifies particles X_k around X_i in the first pulse that may be considered to move in the same manner as particle X_i . The radius T_q arises from the assumption that the movement of X_k particle in the neighboring of X_i particle within a radius T_n is similar to those that of particle X_i , and it restricts the candidate particles Y_l corresponding to particles X_k in the first pulse.

4.2 Tracking procedure of match probability algorithm

The pairing procedure of the match probability algorithm using the above parameters operates as follows. The candidate particles Y_j in the second pulse, corresponding to particle X_i in the first pulse, are determined by the parameter T_m . For X_i , the probability P_{ij} represents the probability of the particle i in the first pulse matching the particle j in the second pulse; the corresponding no-match probability is P_i^* . The total probability has to satisfy the following condition.

$$\sum_j P_{ij} + P_i^* = 1 \tag{5}$$

The initial values for the probabilities are given by

$$P_{ij}^{(0)} + P_i^{*(0)} = \frac{1}{M+1} \tag{6}$$

where M is the number of possible match points (Y_j) in the second pulse within a radius T_m . The superscript denotes the number of iterations.

In the second step, the match probability is updated by neighboring particles X_k , satisfying the quasi-solidity assumptions (3) and (4). The iteration equation is expressed as

$$\tilde{P}_{ij}^{(n)} = A \cdot P_{ij}^{(n-1)} + B \cdot \sum_k \sum_l P_{kl}^{(n-1)} \tag{7}$$

where $A (<1)$ and $B (>1)$ are constants to differentially weight each term and they were estimated as 0.3 and 3.0 by a trial-and-error method, respectively. These constants affect the speed of convergence depending on the concentration of particles and the condition of neighboring particles. The tilde denotes a non-normalized probability value. The non-normalized probability in Eq. (7) should be normalized to satisfy Eq. (5); this is obtained using

$$P_{ij}^{(n)} = \frac{\tilde{P}_{ij}^{(n)}}{\sum_j \tilde{P}_{ij}^{(n)} + P_i^{*(n-1)}} \tag{8}$$

$$P_i^{*(n)} = \frac{P_i^{*(n-1)}}{\sum_j \tilde{P}_{ij}^{(n)} + P_i^{*(n-1)}}$$

After successful iterative convergence, the point Y_j in the second pulse with the largest match probability value is selected as the same particle X_i in the first pulse.

5. Results of Particle Sizes and Velocities

The results of particle velocity extraction are shown in Fig. 9. Figure 9(a) represents the original doubly exposed spray droplet image, and Fig. 9(b) shows droplets in the first pulse only. Figure 9(c) is obtained by subtracting the droplets in the first pulse (Fig. 9(b)) from the binarized image of Fig. 9(a), which results in an image of the droplets in the second pulse only.

The final velocity vectors of the individual droplets are shown in Fig. 9(d). There exist 79 droplets in Fig. 9(b) (first pulse) and 112 droplets in Fig. 9(c) (second pulse). The number of droplets in the first pulse was intentionally lower than that in the second pulse to reduce a matching error and the calculation time required by the particle tracking algorithm. So, 191 droplets were recognized as droplets among a total of 231 droplets in Fig. 9(a), resulting in 82.7% recognition rate. Among the recognized droplets, 69 droplets in the first pulse were paired with droplets in the second pulse, which represented a particle tracking rate of 87.3%. This result ensures that the match probability algorithm still works well even for large particles like droplets in sprays even though it was originally developed for small tracers to measure fluid flow field.

The prerequisite condition for the particle pairing algorithm to produce good pairing results is that both particles at two times must exist. That's why the velocity extractions of relatively large droplets were satisfactory whilst there exist non-paired small droplets. Small droplets are easy to be lost during the binarization process because they usually possess inadequate gray level intensities, and therefore, it is difficult to determine whether the small droplets are present in the first or second pulses. To solve this problem, images resolution should be high enough to allow the intensities of the small particles to reach the level of the large particles, which results in too small a field of view. Therefore, adequate magnification of the spray region should be selected after considering the field of view required and the distribution of droplet sizes.

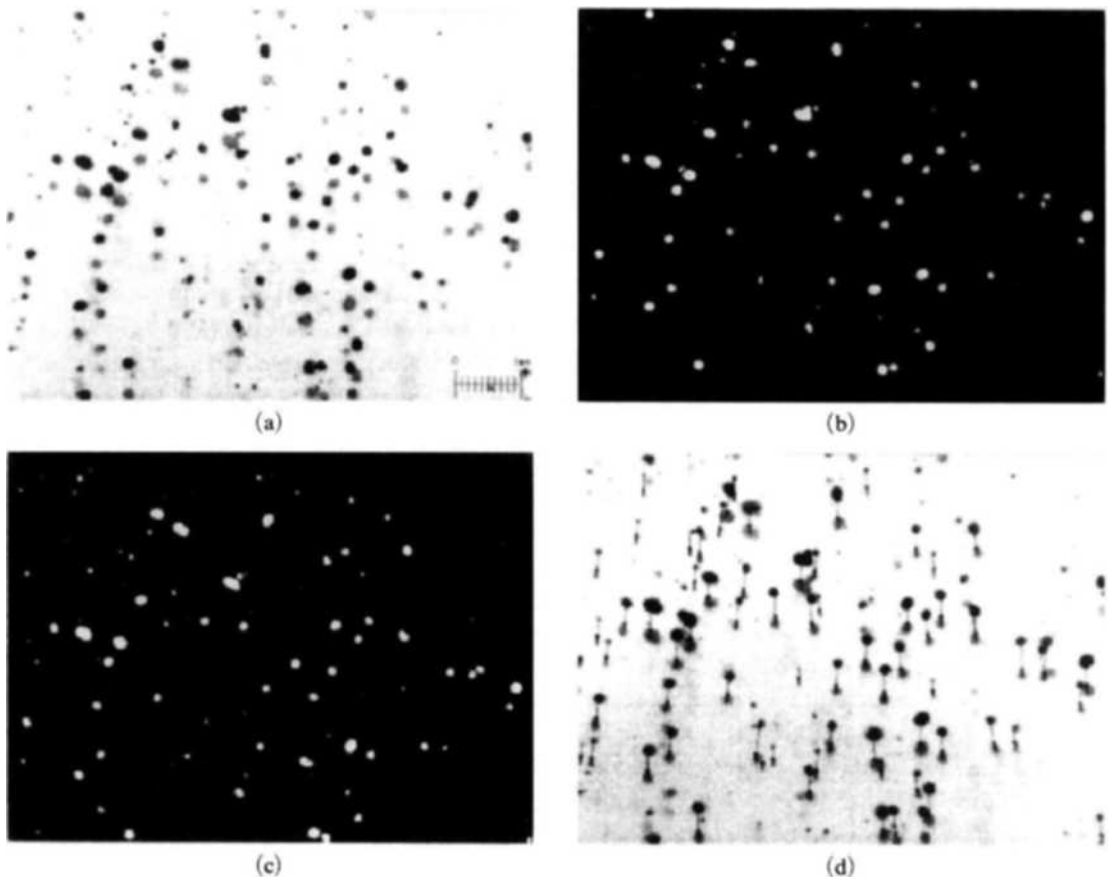


Fig. 9 Droplet velocity extraction from double exposure single frame image

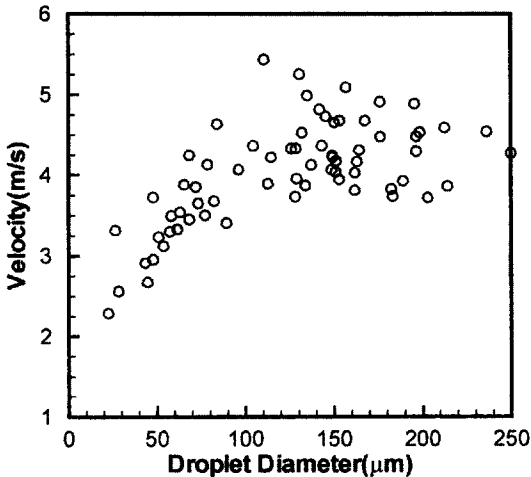


Fig. 10 Distributions of sizes and velocities of droplets

The distributions of sizes and velocities of all processed droplets is shown in Fig. 10, which shows the trend typical of such measurements in sprays, namely, that smaller droplets tend to have lower velocities. The smallest droplet size was $20\ \mu\text{m}$, which indicates that most sprays can be investigated using the described method. The mean diameter and velocity of droplets were $124.33\ \mu\text{m}$ and $4.03\ \text{m/s}$, respectively.

6. Conclusion

In this study, the sizes and velocities of droplets in sprays were measured by an optical imaging method using the digital images of local spray regions. Double-exposure, single-frame spray images with short pulse intervals were captured using an image capturing system. An image processing program was developed for the measurements of the sizes and positions of individual particles including separation of the overlapped particles and particle tracking and pairing at two instances. The morphological method based on the watershed segmentation as well as separation using the perimeter and the convex hull of the image was adopted sequentially to recognize and separate overlapping particles. Utilization of both methods produced better results in separation especially for the multiple

or heavily-overlapped particles. The match probability method was adopted for particle tracking and pairing after identifying the positions of individual particles; and it produced good matching results even for large particles like droplets in sprays. Therefore, the developed optical imaging method could provide a reliable way of analyzing the motion and size distribution of droplets produced by various sprays and atomization devices.

Acknowledgment

This work was supported by a grant No. R05-2000-000-00297-0 from the Basic Research Program of the Korea Science and Engineering Foundation.

References

- Adrian, R. J., 1991, "Particle-Imaging Technique for Experimental Fluid Mechanics," *Ann. Rev. Fluid Mech.*, Vol. 23, pp. 261~301.
- Baek, S. J. and Lee, S. J., 1996, "A New Two-frame Particle Tracking Algorithm using Match Probability," *Experiments in Fluids*, Vol. 22, pp. 23~32.
- Ballard, D. H. and Brown, C. M., 1982, *Computer Vision*, Prentice-Hall, pp. 195~225.
- Crida, R. C. and Jager, G., 1997, "An Approach to Rock Size Measurement based on a Model of Human Visual System," *Minerals Engineering*, Vol. 10, No. 10, pp. 1085~1093.
- Gonzalez, R. C., Woods, R. E., 1992, *Digital Image Processing*, Addison-Wesley Pub.
- Kim, J. Y., Chu, J. H. and Lee, S. Y., 1999, "Improvement of Pattern Recognition Algorithm for Drop Size Measurement," *Atomization and Sprays*, Vol. 9, No. 3, pp. 313~329.
- Kim, J. Y., 2000, "Study of Internal Flow Characteristics and Atomization Performance of Effervescent Atomizers," Ph.D. Thesis, KAIST, Korea.
- Kim, Y. D., Lee, S. Y. and Chu, J. H., 2001, "Separation of Overlapped Particles Using Boundary Curvature Information," *Proceedings of the 6th Annual Conference on Liquid Atomi-*

zation and Spray Systems (ILASS-Asia 2001), pp. 259~264.

Kim, Y. D. and Lee, S. Y., 2002, "Application of Hough Transform to Image Processing of Heavily Overlapped Particles with Spherical Shapes," *Atomization and Sprays*, Vol. 12, pp. 451~461.

Koh, K. U. and Lee, S. Y., 2000, "Determination of Background Gray-level for Accurate Measurement of Particles in Using Image Processing Method," *Transactions of the KSME*, Vol. 24, No. 4, pp. 599~607 (in Korean).

Koh, K. U., Kim, J. Y., and Lee, S. Y., 2001, "Determination of In-focus Criteria and Depth of Field in Image Processing of Spray Particles," *Atomization and Sprays*, Vol. 11, pp. 317~333.

Kruis, F. E., Denderen, J. V., Burrman, H. and Scarlett, B., 1994, "Characterization of Agglomerated and Aggregated Aerosol Particles Using Image Analysis," *Part. Part. Syst. Charact.*, Vol. 11, pp. 426~435.

Labonte, G., 2000, "On a Neural Network that Performs an Enhanced Nearest-neighbour Matching," *Pattern Analysis & Applications*, Vol. 3, pp. 267~278.

Lecuona, A., Rodriguez, P. A., and Zequeira, R. I., 2000, "Volumetric Characterization of Dispersed Two-phase Flows by Digital Image An-

alysis," *Meas. Sci. Technol.*, Vol. 11, pp. 1152~1161.

Lee, S. Y., Park, B. S. and Kim, I. G., 1991, "Gray Level Factors Used in Image Processing of Two-Dimensional Drop Images," *Atomization and Sprays*, Vol. 1, No. 4, pp. 389~400.

Nishino, N., Kato, H. and Torii, K., 2000, "Stereo Imaging for Simultaneous Measurement of Size and Velocity of Particles in Dispersed Two-Phase Flow," *Measurement Science and Technology*, Vol. 11, pp. 633~645.

Otsu, N., 1979, "A Threshold Selection Method from Gray-Level Histograms," *IEEE Transactions on Systems, Man, and Cybernetics*, Vol. 9, No. 1, pp. 62~66.

Shen, L., Song, X., Murai, Y., Iguchi, M., and Yamamoto, F., 2001, "Velocity and Size Measurement of Falling Particles with Fuzzy PTV," *Flow Measurement and Instrumentation*, Vol. 12, pp. 191~199.

Sonka, M., Hlavac, V. and Boyle, R., 1999, *Image Processing, Analysis and Machine Vision*, Brooks/Cole Pub. .

Sudheer, K. P. and Panda, R. K., 2000, "Digital Image Processing for Determining Drop Sizes from Irrigation Spray Nozzles," *Agricultural Water Management*, Vol. 45, pp. 159~167.